IEEE Access
Multidisciplinary | Rapid Review | Open Access Journal

Received February 13, 2019, accepted March 24, 2019, date of publication April 1, 2019, date of current version April 15, 2019.

Digital Object Identifier 10.1109/ACCESS.2019.2908422

Improved Car-Following Strategy Based on Merging Behavior Prediction of Adjacent Vehicle From Naturalistic Driving Data

YINGSHI GUO, QINYU SUN, RUI FU, AND CHANG WANG
School of Automobile, Chang'an University, Xi'an 710064, China

Corresponding author: Qinyu Sun (sunqinyu@chd.edu.cn)

This work was supported in part by the Changjiang Scholars and Innovative Research Team in University under Grant IRT_17R95, in part by the National Natural Science Foundation of China under Grant 51775053, and in part by the Fundamental Research Funds for the Central Universities under Grant 310822151028.

ABSTRACT As the fundamental control strategy of intelligent vehicles, car-following control directly affects vehicle performance. In practical driving, drivers usually predict the behavior of vehicles in the adjacent lane before modulating the driving strategy of the host vehicle. Therefore, an adaptive cruise control (ACC) system should be equipped with the practical ability to predict the following target in advance to improve the safety and acceptability of the intelligent control strategy. In this paper, a car-following strategy based on merging prediction of adjacent vehicles is developed from the results of naturalistic on-road experiments. Based on analysis of merging behavior parameters, the Fisher discriminant method is employed to establish a merging behavior prediction model of adjacent vehicles. Then, the desired spacing car-following model is ameliorated by the proposed merging prediction model. The simulation results of the proposed car-following strategy with different cut-in scenes indicate that the prediction model could forecast two kinds of merging behavior 2 s in advance, and the prediction accuracy rate reaches 88% and 90%, respectively. The improved car-following model could allow for smoother vehicle manipulation, thus enhancing safety and ride comfort. The results provide a reference for improving intelligent vehicle control algorithms and enhancing the acceptability of intelligent systems.

INDEX TERMS Car-following, merging behavior prediction, desired spacing model, Fisher discriminant method.

I. INTRODUCTION

Car-following control, as a fundamental control strategy of intelligent vehicles [1], has developed progressively and has been popular in advanced driving assistant systems (ADAS) to improve driving safety and reduce driver load [2]–[4]. During the practical car-following process, the established following condition would be destroyed when a vehicle in the adjacent lane merges abruptly into the host lane. The sudden reduction in distance and change of the relative velocity between the host vehicle and merging vehicle can easily result in traffic conflicts [5]–[7]. However, drivers usually could predict the behavior of vehicles in the adjacent lane before modulating the driving strategy of the host vehicle during practical driving [8]. Similarly, if the merging behavior of adjacent vehicles could be predicted precisely and enable ADAS to implement prompt countermeasures in advance via an intelligent car-following strategy, the deceleration jerk of the host vehicle would be alleviated, and ride comfort and safety would be enhanced.

In actual driving, the car-following strategy of the host vehicle is observably related to the driving behavior of vehicles in the adjacent lane. Variations in host vehicle behavior include the driver's response to the combined stimulus of preceding vehicles in the same lane and parallel vehicles in the adjacent lane [9]. On the basis of research on the influence of vehicles in the adjacent lane on car-following behavior, Gunay [10] developed a car-following model using the longitudinal distance between the preceding vehicle and host vehicle and lateral distance between vehicles in the adjacent lane and the host vehicle. The proposed model indicated that an increase in the lateral distance would result in a reduction

The associate editor coordinating the review of this manuscript and approving it for publication was Muhammad Awais Javed.

in the following distance between preceding vehicles and the host vehicle. Elusion was the host vehicle's primary option when confronted with persistent pressure from vehicles in the adjacent lane. In other words, the host vehicle driver would maintain psychological comfort by increasing lateral distance with the adjacent vehicle. In the case of insufficient space for lateral elusion, the host vehicle would decelerate and enhance the longitudinal distance to compensate for interference from the adjacent vehicle. Ponnu and Coifman [11] proposed the concept of 'sympathy of speeds' on the basis of research on the relative velocity between the host vehicle and vehicles in the adjacent lane. The study revealed that drivers usually adopted a larger following distance when the relative speed between the host vehicle and adjacent vehicle was large. Lei and Huapu [12] established a comprehensive model of vehicle behavior using a combination of the car-following model, lane change model, and influence of the adjacent vehicle. The research results indicated that the driver would regulate the velocity when the adjacent vehicle either reached the alert distance or possessed higher velocity than the host vehicle. The above studies demonstrate that drivers usually would predict the behavior of vehicles in the adjacent lane before modulating the driving strategy of the host vehicle. Therefore, for the sake of improving the acceptability and safety of the adaptive cruise control (ACC) system, an intelligent car-following strategy should possess the capacity to transform the control strategy based on behavior prediction of adjacent vehicles.

In recent years, many scholars have pursued various approaches to improve the ride comfort and safety performance of ACC systems using cut-in scenes [13]–[16]. By recognizing the target vehicle's motion state, the performance of car-following control strategies has been improved greatly. Schmied *et al.* [17] proposed a robust adaptive cruise control method to improve ride comfort in the ACC system. The proposed model employed model predictive control (MPC) to solve an optimal control problem in a receding horizon manner by analyzing the lane change behavior of the surrounding traffic participants. Also, simulation results with different scenes demonstrated that robust control, when considering lane change behavior, effectively improved driving comfort and exerted positive effects on traffic flow stability. Li *et al.* [18] proposed a novel vehicular ACC system to comprehensively address issues of tracking capabilities, fuel economy, and desired driver response. By considering driver dynamic car-following characteristics, the model provided substantial benefits for satisfying desired driver behavior. Moon *et al.* [19] proposed a primary target selection algorithm for the ACC system based on analyzing the state transitions of neighboring vehicles. Ararat modified the primary car-following algorithm according to the collision warning algorithm when considering human factors and the motion of surrounding vehicles. In brief, the driving behaviors of surrounding vehicles has been a pivotal kernel in designing car-following control methods. However, present control strategies are mainly based on the results of driving behavior recognition of surrounding vehicles; strategy exploitations according to the results of driving behavior prediction (i.e., merging behavior prediction) remain sparse. In reality, the sooner driving intentions are caught, the easier it is to enhance car-following strategies.

Models of merging behavior prediction have been the focus of numerous empirical studies that have investigated different traffic environments. Deo and Trivedi [20] established a long–short-term memory (LSTM) model for motion prediction of surrounding vehicles on freeways. The model took a vehicle's historical trajectory coordinates as input, and merging behavior was predicted by analyzing the distribution probability of the vehicle's trajectory coordinate at the next moment. Fuzzy control logic was used by Moon *et al.* [21] to predict the merging behavior of surrounding vehicles. The logic insisted that an adjacent vehicle would prefer to perform merging behavior when the lateral distance between the host vehicle and adjacent vehicle was small and the lateral relative velocity was large. Vogel *et al.* [22] used a fuzzy support vector machine (FSVM) method to predict merging behavior, and model characteristic parameters were determined as the host vehicle velocity, longitudinal and lateral distance between the host vehicle and adjacent vehicle, relative longitudinal and lateral velocity between the host vehicle and adjacent vehicle, relative longitudinal and lateral acceleration between the host vehicle and adjacent vehicle. Yaping *et al.* [23] proposed a semantic-based intention and motion prediction (SIMP) method to forecast merging intentions by employing a deep neural network. Through comparison with the support vector machine (SVM) method, the established model could predict the merging intention of an adjacent vehicle approximately 2 s in advance, and the prediction accuracy was much higher than with the SVM model. Gadepally *et al.* [24] established a mixed-state model by coupling driver decision making with vehicle dynamics, and a hidden Markov model (HMM) was employed to predict driver behavior by tracking the continuous state of the target vehicle. However, current studies have mainly concentrated on the merging behavior prediction of the host vehicle, the prediction models for surrounding vehicles are scarce. In addition, the performance, especially by leveraging prediction results to improve car-following strategies, also warrants investigation.

In an attempt to precisely predict the merging behavior of adjacent vehicles and promptly modulate the car-following strategy of the host vehicle, this study analyzed the behavior of a vehicle in the adjacent lane that merged into the host lane during the car-following process on a freeway. By exploiting the appropriate kinestate parameters of the host vehicle and surrounding vehicles, a prediction model to forecast the merging behavior of adjacent vehicles was established. Then the existing desired spacing car-following model was ameliorated on the basis of the prediction results. In order to verify the effectiveness of the proposed strategy, different cut-in scenes were designed to further explore the safety and ride comfort of the car-following strategy. The

FIGURE 1. Components of the test vehicle platform.

remainder of this paper is organized as follows. The characteristic parameters of merging behavior are analyzed and determined in Section II. A merging prediction model for the adjacent vehicle, using the Fisher discriminant method, is established in Section III. Simulation results and analysis are reported in Section IV. Finally, conclusions are presented in Section V.

II. CHARACTERISTIC PARAMETERS ANALYSIS AND SELECTION

A. NATURALISTIC DRIVING EXPERIMENT

In order to collect the authentic merging behavior data during the actual car-following process, naturalistic driving experiments were implemented to support the prediction model establishment of the merging behavior. A total of 17 experienced drivers (15 men, 2 women) were recruited to participate in naturalistic driving experiments. Participants were between the age of 27 and 48 years old with an average age of 34.7 years. All participants had valid driving licenses and driving experience ranging from 3 to 23 years (M= 8.4 years). Each participant was physically healthy, and none had been involved in a severe traffic accident within the past 3 years. For the sake of acquisition of the authentic merging behavior data, an integrated data-gathering platform using a real vehicle and common sensors was developed for this study. The test vehicle and pivotal devices are shown in Fig. 1. A millimeter-wave radar was used to acquire the relative velocity and relative distance between the host vehicle and surrounding vehicles. A video monitoring system was employed to calibrate time windows and record applicable merging behavior of adjacent vehicles. The GPS device provided geographical positions of the host vehicle. Relevant parameters of the host vehicle were collected via a controller area network (CAN) acquisition card. All acquired data were finally encoded in an industrial control computer. A full closed two-way, 6-lane freeway was selected to accomplish the naturalistic driving experiments. The total mileage driven exceeded 5000 km.

B. DATA DESCRIPTION

According to practical merging data during naturalistic driving experiments, we divided merging behavior into three

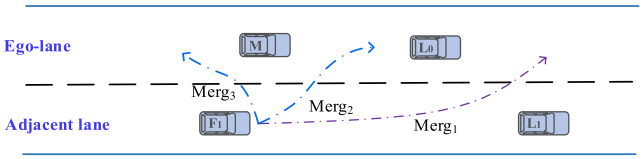

FIGURE 2. Schematic diagram of merging behaviors of adjacent vehicle.

categories. The schematics of different merging behavior categories are presented in Fig. 2, where M represents the host vehicle, L_0 represents the preceding vehicle in the same lane as the host vehicle, and F_1 represents the vehicle in the adjacent lane. During the car-following process between host vehicle M and preceding vehicle L_0, vehicle F_1 exceeded vehicle L_0 and merged in front of vehicle L_0 in the first merging behavior case, recorded as $Merg_1$. In the second case, vehicle F_1 merged between vehicle M and vehicle L_0,recorded as $Merg_2$. In the third case, vehicle F_1 merged after vehicle M, recorded as $Merg_3$. Based on analysis of actual merging behavior data, $Merg_3$ was relatively scarce and exerted negligible influence on vehicle M. Therefore, this study emphasizes $Merg_1$ and $Merg_2$.

During the whole naturalistic driving experiments, all participants were just informed of the initial points and destinations; no other instructions were given. Participants could navigate the host vehicle allodially under the premise of obeying the rules and ensuring driving safety. For offline extraction of car-following data and merging behavior data, we defined data screening principles in advance, and the detailed descriptions are provided below.

1) The velocity range of the test vehicle ranged from 60 km/h to 100 km/h. A velocity below 60 km/h did not reflect normal freeway driving, and such data were removed. Limits of the freeway sections were 100 km/h and 110 km/h. A velocity more than 100 km/h was rare, and only the data with a host vehicle velocity below 100 km/h were selected.
2) Determining the car-following state was the premise of acquiring the merging behavior data. Literatures[25] and [26] deemed 5 s and 6 s of headway time as the demarcation point between free driving and car-following behavior. In this study, we confirmed 5 s of headway time as the demarcation value. Therefore, scenes with a time headway of less than 5 s and sustained for more than 10 s were defined as the car-following stage.
3) The moment at which the turn signal was activated was the criterion for merging intention judgment; the moment of lateral displacement was regarded as the criterion for merging initiation judgment. According to videos recorded by the video monitoring system, the initial merging intention of vehicle $F_1$was taken as the turn-signal starting time. The terminative merging intention was confirmed as the moment that vehicle F_1began to make a lateral offset. Then, continuous data

from 1-2 s before the moment of merging intention termination were intercepted for characteristic parameter analysis.

On the basis of the above principles, we finally selected 50 instances of $Merg_1$behavior and 50 instances of$Merg_2$ behavior. A total of 800 groups of $Merg_1$ behavior samples and 800 groups of $Merg_2$ behavior samples were included. Among them, data of $Merg_1$, with the velocity of vehicle M within the range of [60, 80) km/h, reached 370 groups, and velocity situated in the range of [80, 100) km/h reached 430 groups. Data of $Merg_2$ with the velocity of vehicle M within the range of [60, 80) km/h reached 320 groups, and velocity situated in the range of [80, 100) km/h reached 480 groups. The neighborhood smoothing filter method was applied to denoise acquired data prior to analysis.

C. CHARACTERISTIC PARAMETERS ANALYSIS OF MERGING BEHAVIOR

Selecting applicable characteristic parameters is a pivotal kernel to establish a prediction model of merging behavior. Appropriate parameter selection can effectively simplify the prediction model and improve the accuracy of merging behavior prediction. In this study, the velocity of host vehicle V_M, longitudinal distance between the host vehicle and preceding vehicle d_1, headway time between the host vehicle and preceding vehiclet_1, relative velocity between the host vehicle and preceding vehicle V_{ML}, longitudinal distance between the host vehicle and adjacent vehicle d_2, headway time between the host vehicle and adjacent vehicle t_2, relative velocity between the host vehicle and adjacent vehicle V_{MF}, acceleration of host vehicle a_0, acceleration of preceding vehicle a_1, and acceleration of adjacent vehicle a_2 were preliminarily selected as characteristic parameters. All parameters could be deduced from data collected by the test platform. However, the acceleration of a_0, a_1, and $a_2$demonstrated negligible differences in the two velocity intervals for $Merg_1$ behavior and $Merg_2$ behavior, respectively, and we first eliminated these three accelerations from the candidate parameters. Then, linear correlation analysis [27], [28] was performed on the remaining seven parameters (i.e., V_M, t_1, t_2, V_{ML}, V_{MF}, d_1, and d_2), and the correlation coefficient matrix is depicted in Fig. 3.

As shown in Fig. 3, different colors in the elliptical blocks depicted the discrepant degree of linear correlation between each pair of parameters. The size of elliptical blocks indicated the strength of the correlation, and the long axis direction indicated that variables were positively correlated. The value of the correlation coefficient between each parameter pair was directly shown in the elliptical blocks, and the larger the value, the higher the correlation. The value of the linear correlation coefficients between d_2 and t_2 and d_1 and t_1 were largest, reaching 0.98 and 0.95, respectively. In addition, the values between d_1 and V_M and d_2 and V_M were also strong, reaching 0.57 and 0.61, respectively. Collectively, the value of the linear correlation coefficients between V_{ML} and other parameters as well as V_{MF} and

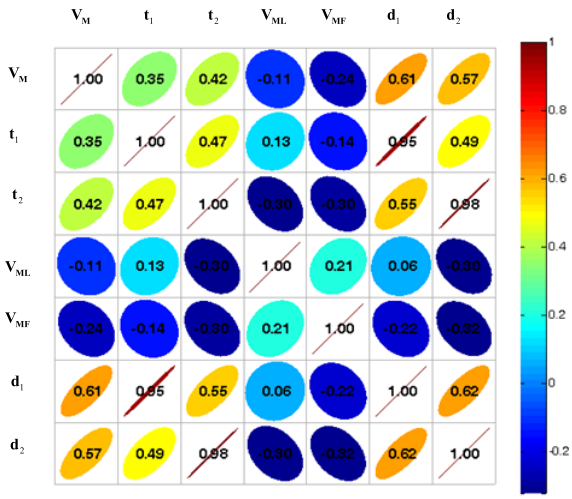

FIGURE 3. Correlation coefficient matrix.

other parameters were all under 0.4. Hence, the parameters of V_M, V_{ML}, V_{MF}, t_1,and t_2 were retained. On the contrary, the parameters of d_1 and d_2 were eliminated.

In order to further filter out characteristic parameters, multicollinearity diagnosis based on the variance inflation factor (VIF) [29], [30] of each parameter was employed in this study. Multiple linear regression was performed for the remaining variables for parameter X_i, and the model determination coefficient R_i^2

was calculated as follows.

$$R_i^2 = 1 - \frac{SSE_i}{SST_i} \tag{1}$$

where SSE_i is the square sum of the residuals, and SST_i is the sum of squares of the total deviation.

The VIF of parameter i can be calculated as

$$VIF_i = 1 - \frac{1}{R_i^2} \tag{2}$$

When diagnosing potential multicollinearity on the basis of VIF values, the diagnostic criterions were as follows: $VIF<5$ indicated no or weak multicollinearity; $5 \leqslant VIF \leqslant 10$ indicated a moderate degree of multicollinearity; and $VIF> 10$ indicated high multicollinearity, which should be eliminated. Next, we calculated respective VIF values for seven variables V_M, t_1,t_2, V_{ML}, V_{MF}, d_1, and d_2, respectively. The results were as follows: $VIF_7 = [12.6140, 79.3822, 101.7321, 1.2747, 1.1917, 114.6772, 128.3634]$. Apparently, severe multicollinearity existed when the parameters of $d_1$and d_2 were not eliminated. And results without d_1 and d_2 indicated that $VIF_5 = [1.2823, 1.4933, 1.7139, 1.2515, 1.1387]$. The results demonstrated that the parameters of V_M, t_1, t_2, V_{ML}, and V_{MF} possessed weak multicollinearity, and the parameters of $d_1$and$d_2$should be eliminated. In addition, the four parameters t_1, t_2, V_{ML}, and V_{MF}, along with data of$Merg_1$ and $Merg_2$ behavior under the velocity intervals of [60, 80) km/h and [80, 100) km/h, are listed respectively in Tables 1 and 2.

TABLE 1. Parameter values of t_1,t_2,V_{ML},V_{MF}within [60, 80) km/h.

parameter	t_1 (s)		t_2 (s)		V_{ML} (m/s)		V_{MF} (m/s)	
Types	$Merg_1$	$Merg_2$	$Merg_1$	$Merg_2$	$Merg_1$	$Merg_2$	$Merg_1$	$Merg_2$
Mean	2.0	2.7	1.1	1.1	-1.15	1.57	3.19	1.23
Maximum	3.3	5.0	1.9	2.6	1.80	6.45	8.13	9.52
Minimum	1.2	1.1	0.5	0.3	-4.16	-2.48	-1.12	-3.77
S.D.	0.6	1.0	0.4	0.6	1.48	2.00	2.62	3.54

TABLE 2. Parameter values of t_1,t_2,V_{ML},V_{MF}within [80, 100) km/h.

parameter	t_1 (s)		t_2 (s)		V_{ML} (m/s)		V_{MF} (m/s)	
Types	$Merg_1$	$Merg_2$	$Merg_1$	$Merg_2$	$Merg_1$	$Merg_2$	$Merg_1$	$Merg_2$
Mean	2.8	3.0	2.2	1.3	-2.86	1.81	2.17	0.62
Maximum	4.3	5.0	3.4	3.5	1.37	6.60	6.26	5.05
Minimum	1.4	1.5	0.5	0.3	-9.18	-4.57	-1.95	-7.04
S.D.	0.7	0.9	0.7	0.7	2.78	2.48	2.01	2.81

By comparison with Tables 1 and 2, the t_1 and V_{ML} values of $Merg_2$ behavior were larger than $Merg_1$ behavior under the two different velocity intervals. The V_{MF} values of $Merg_2$ behavior were smaller than for$Merg_1$ behavior. As for t_2, the trend between $Merg_1$ and $Merg_2$ with two velocity intervals was inconsistent. In conclusion, by comprehensive consideration of the characteristic distribution and collinearity of the parameters, V_M, t_1, V_{ML}, and V_{MF} were ultimately selected as characterization parameters of merging behaviors.

III. MERGING PREDICTION MODEL ESTABLISHMENT OF ADJACENT VEHICLE

A. MERGING PREDICTION MODEL ESTABLISHMENT

Prediction model establishment has been the objective of abundant empirical researches that have investigated different machine learning methods (i.e., Bayesian classification, HMM, Gaussian classification, SVM, and artificial neural networks) and deep learning methods [31], [32]. However, in actual use for uncomplicated driving behavior forecasting, under the premise that the prediction accuracy is basically the same, the simpler the model, the more efficient and practical it will be. Hence, discriminant analysis method was used in this study to establish the merging prediction model. Discriminant analysis aims to distinguish categories of unknown samples using the existing sample classification. The basic idea is to discriminate category attributes of unknown sample types according to the constructed discriminant function and discriminant criterion according to the extracted samples [33]. The Fisher discriminant method decreases the dimensions of high-dimensional independent variables through projection; thus, data from different groups can be separated as much as possible, and discrepancies in data from the same group are as limited as possible to classify them into a low-dimensional space. In addition, the Fisher discriminant method has no requirement regarding data distribution type or magnitude of the variance and possesses a range of uses [34]. In this study, pivotal procedures of establishing the discriminant function and discriminant criterion are as follows.

We first defined kp-dimensional populations G_1, G_2,..., G_k, and samples extracted from the population were denoted as $x_{i1}, x_{i2},\ldots, x_{in}$ $(i = 1,2,\ldots, k)$. The total number of samples, the mean of samples, and mean values of respective samples were denoted as $n = \sum_{i=1}^{k} n_i$, $\bar{x} = \frac{1}{n}\sum_{i=1}^{k}\sum_{j=1}^{n_i} x_{ij}$ and $\bar{x_i} = \frac{1}{n_i}\sum_{j=1}^{n_i} x_{ij}$. Then, we assumed that the projection direction was $\mathbf{a} = (a_1, a_2, \ldots, a_p)^{\mathbf{T}}$, x_{ij} was projected on $\mathbf{a}$, and $y_{ij} = \mathbf{a}^{'} x_{ij} (i = 1, 2, \ldots, k; j = 1, 2, \ldots, n_i)$. Therefore, the mean values of the projection data were $\bar{y} = \frac{1}{n}\sum_{i=1}^{k}\sum_{j=1}^{n_i} y_{ij} = \mathbf{a}^{'}\bar{x}$, and $\bar{y}_i = \mathbf{a}^{'}\bar{x}_i$. The sum of squares of the differences between groups of $y_{ij} (i = 1, 2, \ldots, k; j = 1, 2, \ldots, n_i)$ was denoted as SS_G. The deviation squared sum of squares in the group was denoted as SS_E, as shown in (3) and (4).

$$\mathbf{SS_G} = \sum_{i=1}^{k} n_i(\bar{y}_i - \bar{y})^2 = \sum_{i=1}^{k} n_i(\mathbf{a}^{'}\bar{x}_i - \mathbf{a}^{'}\bar{x})^2 \tag{3}$$

$$\mathbf{SS_E} = \sum_{i=1}^{k}\sum_{j=1}^{n_i}(y_{ij} - \bar{y}_i)^2 = \sum_{i=1}^{k}\sum_{j=1}^{n_i}(\mathbf{a}^{'}x_{ij} - \mathbf{a}^{'}\bar{x}_i)^2 \tag{4}$$

Here, we defined $\mathbf{B} = \sum_{i=1}^{k} n_i(\bar{x}_i - \bar{x})(\bar{x}_i - \bar{x})^{\mathbf{T}}$, $\mathbf{E} = \sum_{i=1}^{k}\sum_{j=1}^{n_i}(x_{ij} - \bar{x}_i)(x_{ij} - \bar{x}_i)^{\mathbf{T}}$, hence the statistic can be denoted as $\mathbf{F} = \frac{\mathbf{SS_G}/(k-1)}{\mathbf{SS_E}/(n-k)} = \frac{\mathbf{a}^{'}\mathbf{Ba}/(k-1)}{\mathbf{a}^{'}\mathbf{Ea}/(n-k)}$, $\Delta(\mathbf{a}) = \frac{\mathbf{a}^{'}\mathbf{Ba}}{\mathbf{a}^{'}\mathbf{Ea}}$. If the projection of k groups data was significantly different, then$\mathbf{F}$ or $\Delta(\mathbf{a})$ should be sufficiently large. Thus, if we obtain the maximum point of $\Delta(\mathbf{a})$, then we can get a projection direction $\mathbf{a}$ and constrain $\mathbf{a}$ as a unit vector. The maximum value of $\Delta(\mathbf{a})$ was the largest eigenvalue of $\mathbf{E}^{-1}\mathbf{B}$.

Assuming that all non-zero eigenvalues in $\mathbf{E}^{-1}\mathbf{B}$were arranged as $\lambda_1 \geq \lambda_2 \geq \cdots \geq \lambda_s$, $s \leq min(k-1, p)$, the corresponding unit eigenvectors were $\mathbf{t_1}, \mathbf{t_2}, \ldots, \mathbf{t_s}$, and $\Delta(\mathbf{t_i}) = \frac{\mathbf{t_i^T B t_i}}{\mathbf{t_i^T E t_i}} = \frac{\mathbf{t_i^T}(\lambda_i \mathbf{E t_i})}{\mathbf{t_i^T E t_i}} = \lambda_i (i = 1, 2, \ldots, s)$. Then, the$i$-th discriminant can be calculated by using (5).

$$\mathrm{y_i} = \mathbf{t_i x} (i = 1, 2, \ldots, s) \tag{5}$$

The discriminant efficiency of the$i$-th discriminant was λ_i and the contribution rate of each group was $\frac{\lambda_i}{\sum_{i=1}^{s}\lambda_i} (i = 1, 2, \ldots, s)$. If the total contribution rate of the previous r $(r \leq s)$ discriminants was higher than a threshold (e.g., 85% or more), then the former r discriminants could be used to distinguish the groups well. The former r discriminants were applied to any sample $\mathbf{x}$ and obtained the projection vector $(y_1, y_2, \ldots, y_r)^T$, which was the discriminant vector of $\mathbf{x}$.The former$r$ discriminants were applied to the mean of the i-th group, and the projection vector $(\bar{y}_{i1}, \bar{y}_{i2}, \ldots, \bar{y}_{ir})^T$ was calculated. When the Euclidean distance of the two projection vectors was calculated, the discriminant criterion was as shown in (6).

$$\sum_{j=1}^{r}(y_j - \bar{y}_{ij})^2 = \sum_{j=1}^{r}(y_j - \bar{y}_{hj})^2, \mathbf{x} \in G_i \tag{6}$$

In this study, half of the $Merg_1$ behavior and $Merg_2$ behavior samples were selected as the training set, and the remaining samples were used to verify the prediction model. The mean values of the training data of $Merg_1$ behavior, $Merg_2$ behavior, and all merging behaviors were as follows:

$$\bar{x}^{(1)} = (82.59838, 2.8750, 1.5957, 0.68535)^T \quad (7)$$

$$\bar{x}^{(2)} = (81.18488, 2.4435, -2.08328, 2.6539)^T \quad (8)$$

$$\bar{x} = (81.89162, 2.65925, -0.24379, 1.669625)^T \quad (9)$$

After calculation, the eigenvalue was 1.5772, and the contribution rate reached 100%. The discriminant matrix was denoted as y =[0.000157,-0.37794,-0.7794,0.51538], and the corresponding discriminant was

$$Can = 0.00157V_M - 0.37794t_1 - 0.76912V_{ML} + 0.51538V_{MF} \quad (10)$$

The mean values $\bar{x}^{(1)}$ and $\bar{x}^{(2)}$ of $Merg_1$ behavior and $Merg_2$ behavior were substituted into the Fisher discriminant Can; the discriminant mean of $Merg_1$ behavior was 2.0593, and that of $Merg_2$ behavior was -1.9477. In this study, we analyzed the two populations of merging behaviors, and the Euclidean distance was equivalent to the distance in the one-dimensional space. Therefore, the discriminant criterion was equivalent to the value of the discriminant threshold obtained by weighting the number of samples, and the final value was 0.0558.

B. ANALYSIS OF MODEL RESULTS

The scatter plot for the 800 points of training sample data is shown in Fig. 4. The red line in Fig. 4 represents the discriminant criterion 0.0558 (i.e., the discriminant threshold), and the established discriminant criterion can separate the two merging behaviors effectively; only a fraction of sample data could not be distinguished. The prediction result was distinctly more effective for$Merg_1$ behavior, and only sparse data points were determined promiscuously. The normal density function curves for $Merg_1$ behavior and $Merg_2$ behavior on the basis of Fisher discriminant scores obtained from the training samples are shown in Fig. 5. As shown in Fig. 5, the probability density of $Merg_1$ behavior and $Merg_2$behavior

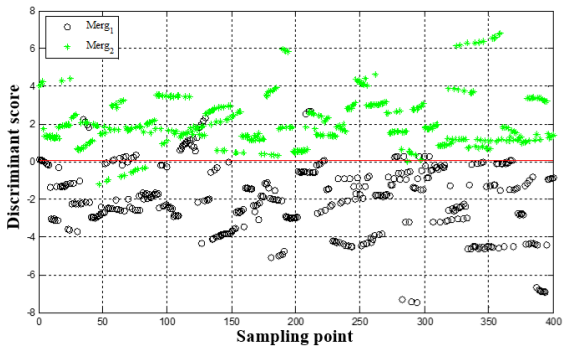

FIGURE 4. Distribution of discriminant scores of training samples.

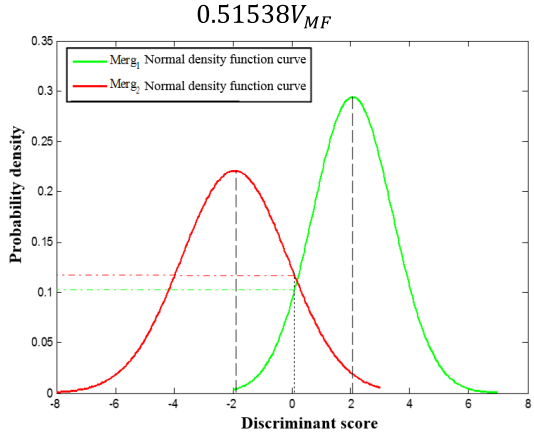

FIGURE 5. Normal density curve for $Merg_1$ and $Merg_2$.

was 0.1 and 0.12, respectively, when the discriminant score was 0.0558. Therefore, in this study, the prediction accuracy of$Merg_1$ behavior was roughly 90%, and that of $Merg_2$ was approximately 88%.

Finally, the other 800 data points were employed to verify the accuracy of the proposed merging behavior prediction model. The confusion matrix of the prediction model is shown in Table 3. For the 400 samples of $Merg_1$ behavior, 12 samples were incorrectly predicted as $Merg_2$ behavior. For the 400 samples of $Merg_2$ behavior, 43 samples were incorrectly forecasted as $Merg_1$ behavior. Therefore, the prediction accuracy rate of $Merg_1$ behavior reached 97%, and that of $Merg_2$ behavior was 89.3%. The prediction results thus satisfied the requirements of car-following strategy modulation.

TABLE 3. Confusion matrix of prediction model.

From/To	$Merg_1$	$Merg_2$	Total
$Merg_1$	388（97%）	12（3%）	400
$Merg_2$	43（10.7%）	357（89.3%）	400

IV. CAR-FOLLOWING STRATEGY IMPROVEMENT AND SIMULATION

A. EXPECTED SPACING CAR-FOLLOWING MODEL

At present, the safety distance car-following model and expected spacing car-following model have been exploited diffusely in the ACC system. A critical value of headway time between the host vehicle and preceding vehicle is given by the safety distance model during the car-following process. As a safety characteristic of car-following behavior, the critical value of headway time cannot synthetically reflect the driver's car-following characteristics on the freeway. The expected spacing model simulates psychological expectation spacing when drivers are following a preceding vehicle, and the model can more realistically and appropriately reflect driver characteristics via comparison with other car-following models. In this study, an anticipated spacing car-following model proposed in our previous research was employed to

re-design a car-following strategy on the basis of the merging behavior prediction model.

The expected spacing car-following model was established on the basis of naturalistic driving data on the freeway [35]. A detailed description (i.e., the expected spacing formula, maximum spacing formula, minimum spacing formula, and acceleration formula) is shown in (11), (12), (13) and (14).

$$D_{exp}(v) = -263.3 + 10.19v - 0.1143v^2 + 0.0001294v^3 \tag{11}$$

$$D_{max}(v) = -577.2 + 22.5v - 0.2584v^2 + 0.001094v^3 \tag{12}$$

$$D_{min}(v) = -108.2 + 4.738v - 0.05821v^2 + 0.0002407v^3 \tag{13}$$

$$a_n(t+T) = 0.0643 + 0.5084v'(t) \tag{14}$$

where v is the host vehicle velocity, $v'(t)$ is the relative velocity between the preceding vehicle and host vehicle, and T is the driver's reaction time, and here we took the value as 0.8 s in this study.

B. CAR-FOLLOWING MODEL IMPROVEMENT

For common car-following strategies, if the adjacent vehicle were to merge into the host lane, the car-following control of the host vehicle would change the following target from preceding vehicle L_0 (shown in Fig. 3) to adjacent vehicle F_1. However, the following target usually switched at the moment that vehicle F_1crossing the lane. This strategy indicated that the current car-following control strategy could not accurately reflect practical driving behavior on the freeway. The safety, ride comfort, and acceptability were also affected. In this study, the expected spacing car-following model accomplished control of the host vehicle when the host vehicle was in a stable following state. According to the established merging behavior prediction model, the merging behavior of the adjacent vehicle F_1would be forecasted 2 s before the initial lateral distance of the vehicle F_1.

In actual driving, the driver would release the accelerator pedal or make a slight braking upon assessing the lateral distance and relative velocity between the host vehicle and adjacent vehicle after perceiving the merging intention of the adjacent vehicle. In this study, we ameliorated the expected spacing car-following strategy according to authentic driving characteristics. The detailed strategy is as follows. When the merging intention of the adjacent vehicle was forecasted by the proposed prediction model, the throttle and brake pressure of vehicle Mwere each adjusted to zero. If the longitudinal distance between vehicle M and vehicle F_1 was less than the expected spacing, deceleration of 0.5 m/s^2 was imposed to vehicle M. After 0.6 s of lateral deviation (our previous study results demonstrated that merging behavior would be recognized after 0.6 s of lateral deviation [36]) and when the velocity of vehicle F_1 was lower than or equal to the expected velocity of vehicle M, if the spacing between vehicle M and vehicleF_1 was greater than expected, control was implemented according to the expected spacing model, and the following target of the host vehicle was translated to adjacent vehicle F_1. If the distance between vehicle M and vehicle F_1 was less than the expected spacing and the distance continued to decline, vehicle M would sustain deceleration, and the following target of the host vehicle was translated to adjacent vehicle F_1 after vehicle F_1 crossed the lane. Reference [37] indicated that the average duration of merging behavior was 5.6 s; therefore, the improved car-following control strategy could switch the following target 2.2 s in advance compared with the original control strategy. A flow chart of the modified control strategy is illustrated in Fig. 6.

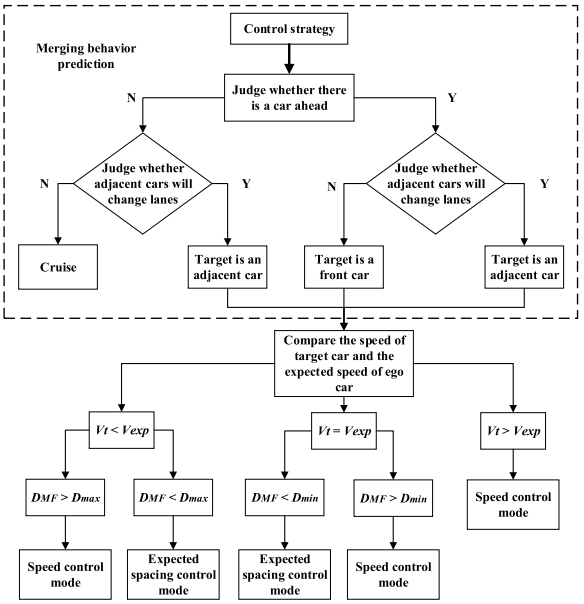

FIGURE 6. Flow chart of modified control strategy.

C. SIMULATION ANALYSIS

For the sake of examining the performance of the ameliorative car-following strategy, PreScan, CarSim, and MATLAB/Simulink were employed to implement co-simulation analysis. In this study, the co-simulation were principally comprised by scenario assumptions, simulation scenario settings, additional sensors addition and control-module operation. PreScan was used to construct different simulation scenarios. By coordinating different virtual sensors, PreScan could also furnish the same real-time kinematic data as our actual acquisition platform. The vehicle dynamic model of our test vehicle was established in CarSim. Moreover, the ameliorative car-following strategy was encoded by MATLAB/Simulink. The following assumptions were made before the co-simulation. Assumed that before adjacent vehicleF_1 merged, host vehicle M had reached a steady car-following state, and preceding vehicle L_0 was always navigating in the host lane; also, the velocity of adjacent vehicle F_1 remained unchanged during the merging process.

In PreScan, we selected a model similar to the test vehicle and set the relevant parameters according to data from the naturalistic driving experiments. The detailed simulation scenario was arranged as follows/. Set the simulation road as a two-way, 6-lane road with a lane width of 3.75 m. The initial velocity of vehicle M was 100 km/h, vehicle $L_0$was always steered at a uniform velocity of 100 km/h, and vehicle F_1navigated uniformly at a velocity of 72 km/h during the whole merging process. The initial spacing between vehicle M and vehicle F_1 was 96 m. According to the results of actual road merging behavior data in China, the duration of merging behavior was set to 3.2 s. Per the national standard, the average deceleration of the ACC system should not be greater than 3.0 m/s^2, and system acceleration should not be greater than 2 m/s^2 [38]. Therefore, the acceleration range of vehicle M was -3 m/s^2 $\leq a_0 \leq$ 2 m/s^2. A TIS distance detection sensor was used to detect the distance, relative velocity, and relative angle between the host vehicle and preceding vehicle. The selected expected spacing model and improved car-following model were each encoded into the Simulink control module.

The co-simulation results for the original expected spacing model and improved car-following strategy are displayed from Fig. 7 to Fig. 10.

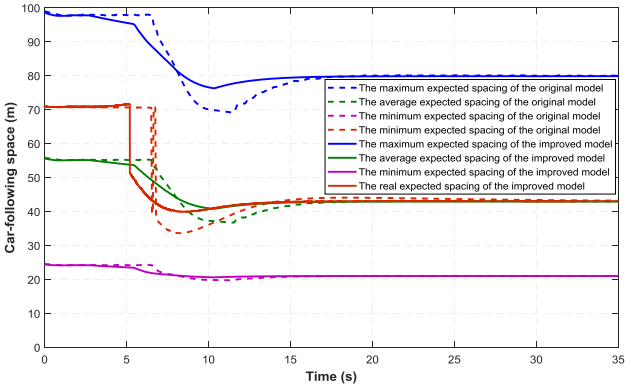

FIGURE 7. Simulation results for car-following space.

Fig. 7 shows the simulation results of the car-following spacing variation compared with the original expected spacing model and improved model, which included the maximum expected spacing, minimum expected spacing, average expected spacing, and actual car-following spacing. As indicated in Fig. 7, the spacing of the two car-following models did not exceed the minimum expected spacing, indicating that the two models demonstrated satisfactory safety. However, the improved model responded earlier to merging behavior than the original model. The inflection points of the curves revealed that the following target had been changed at that moment. All curves derived from the improved model reached the inflection point earlier than those from the original model. In addition, all curves from the improved model possessed higher minimum spacing values than the original model. The minimum spacing of real car-following spacing between the original model and improved model were

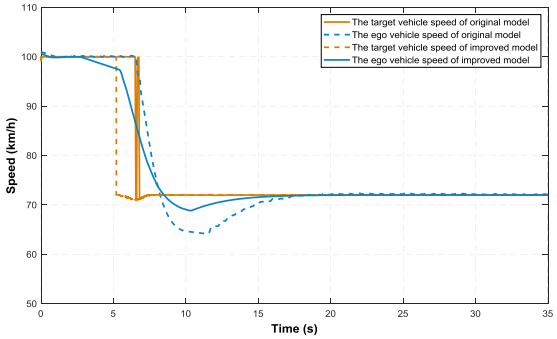

FIGURE 8. Simulation results for host vehicle velocity.

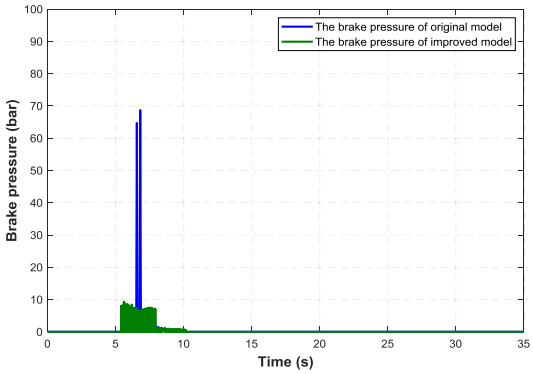

FIGURE 9. Comparison of brake pressure.

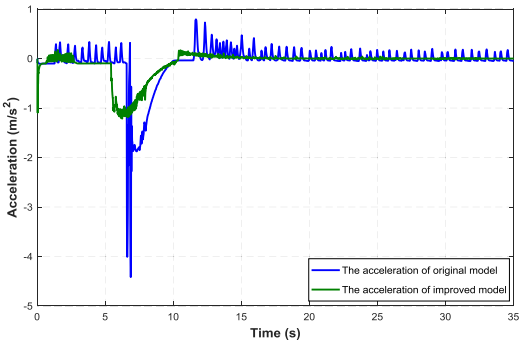

FIGURE 10. Comparison of brake acceleration.

33 m and 40 m, respectively. A higher value of the real car-following spacing implied that the improved model was more secure than the original model.

Fig. 8 presents the simulation results of the host vehicle velocity variation compared with the original expected spacing model and improved model, which included the target velocity and real velocity. As shown in Fig. 8, the inflection points of the curves indicated that the following target had been changed at that moment. The real velocity curve of the improved model had already begun to descend gently before the following target changed. At this stage, the host vehicle had already captured the merging intention of the adjacent vehicle, and the throttle and brake pressure were each adjusted to zero. The host vehicle decelerated naturally

due to rolling resistance and air resistance. Slight deceleration was sustained until the lateral distance of the adjacent vehicle was recognized (0.6 s after lateral deviation). On account of the premature modulation, the real velocity of the improved model transformed more gradually than the curve of the original model. In addition, the minimum velocity of the original car-following model was 64 km/h, whereas that of the improved model was 69 km/h. Hence, the ride comfort was clearly enhanced by the improved model.

Simulation results of brake pressure variation and acceleration variation compared with the original expected spacing model and improved model are pictured in Fig. 9 and Fig. 10, respectively. The brake pressure of the original car-following model had a sudden change at the moment the following target changed, and the maximum brake pressure increased sharply to 70 bar. However, due to the merging intention had been predicted, the improved model braked in advance, and the maximum brake pressure did not exceed 10 bar. The discrepant brake pressure directly affected the acceleration variation of the host vehicle. As shown in Fig. 10, the inflection points of the curves indicated that the following target changed at that moment. The maximum deceleration of the improved model was -1.2 m/s^2, whereas that of the original model reached -4.4 m/s^2. In addition, the maximum acceleration between the improved model and original model was 0.2 m/s^2 and 0.8 m/s^2, respectively. By eliminating deceleration jerk, the host vehicle would be more stable, and ride comfort was enhanced dramatically.

During the merging process, the cut-in velocity of the adjacent vehicle and cut-in distance between the host vehicle and adjacent vehicle each exerted large effects on the host vehicle control. In order to further analyze the performance of the ameliorative car-following strategy, simulation scenarios with different cut-in velocities of the adjacent vehicle and different cut-in distances between the host vehicle and adjacent vehicle were used to test the improved model. A total of 17 simulation scenarios were performed from 10 km/h to 58 km/h at an interval of 3 km/h of the cut-in velocity. From 16 m to 86 m, there were eight simulation scenarios at an interval of 10 m of the cut-in distance. Based on the improved car-following model, a co-simulation study was conducted on different cut-in conditions in the safety range, and results are shown in Figs. 11 and 12.

After the following target changed, the spacing between the host vehicle and adjacent vehicle would continue to on account of the relative velocity difference. A traffic conflict could easily occur when the car-following spacing was less than the minimum safety distance. As shown in Fig. 11, the minimum car-following spacing with different relative velocities and different cut-in spacing were drawn in a 3D contour map. The red part indicated a high probability of collision, and the blue part indicated a low probability of collision. As the relative velocity declined and the cut-in spacing increased, the safer the host vehicle became during the car-following process. The unsafe status (the red part) only occurred in extreme cases. Similarly, maximum deceleration

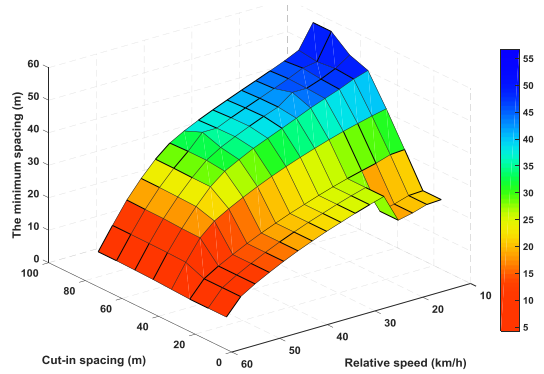

FIGURE 11. Minimum spacing simulation results.

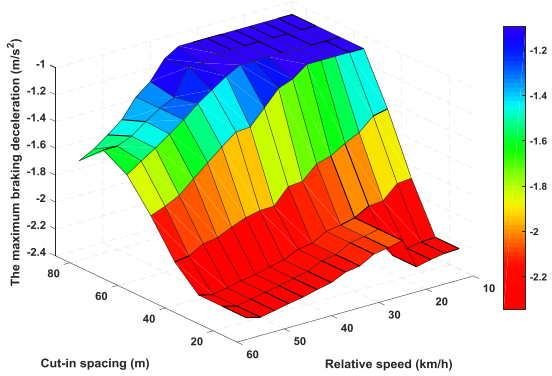

FIGURE 12. Maximum braking deceleration simulation results.

with different relative velocities and different cut-in spacings is shown in Fig. 12. The red part indicated that the host vehicle demonstrated strong deceleration, and the blue part indicated low deceleration. As the relative velocity reduced and the cut-in spacing increased, the lower the deceleration of the host vehicle during the car-following process. The overall deceleration did not exceed -2.5 m/s^2, and high deceleration only occurred in extreme cases. These results demonstrated that the improved model could operate effectively under almost normal cut-in conditions.

V. CONCLUSIONS

The merging behavior prediction of adjacent vehicles plays a substantial role in improving the safety, ride comfort, and acceptability of the intelligent car-following strategy. In this work, an ameliorative car-following strategy based on merging prediction of adjacent vehicles is developed from the results of naturalistic on-road experiments. On the basis of collection and analysis of the kinematic parameters among of the host vehicle, preceding vehicle, and adjacent vehicle; host vehicle velocity, headway time between the host vehicle and preceding vehicle, relative velocity between the host vehicle and preceding vehicle, and relative velocity between the host vehicle and adjacent vehicle are determined to be the characteristic parameters of merging behavior. Then, the Fisher discriminant method is exploited to establish a

merging behavior prediction model on the basis of the four characteristic parameters. Results manifest that the proposed prediction model could forecast the two kinds of merging behavior 2 s in advance. For the two behaviors in which the adjacent vehicle mergers in front of the preceding vehicle and mergers into the gap between the host vehicle and preceding vehicle, prediction accuracy rates reach 90% and 88%, respectively.

In actual car-following behavior on the freeway, a driver would usually release the accelerator or apply the brake slightly upon perceiving the adjacent vehicle's merging intention. In this study, the existing expected spacing car-following model is improved based on the merging prediction model. When the intention of the adjacent vehicle is captured, the throttle releases and the vehicle decelerates by rolling resistance and air resistance. After 0.6 s of the initial lateral displacement, the host vehicle switches the target and enters ACC control. By comparing variations in the host vehicle velocity, car-following spacing, and host vehicle deceleration of the original model and the improved model, simulation results demonstrate that the improved car-following strategy eliminates deceleration jerk, the velocity control is more stable, and the real minimum following spacing increases compared with the original model. The safety, ride comfort, and acceptability of the ameliorative car-following strategy based on the merging prediction model are effectively enhanced. However, some deficiencies exist in this work. Future studies should include more samples with complex traffic environments to train the prediction model and enhance the model portability. In addition, hardware-in-the-loop tests and practical vehicle experiments should implement to verify the performance of the proposed car-following model.

REFERENCES

[1] S. Panwai and H. Dia, "Comparative evaluation of microscopic car-following behavior," *IEEE Trans. Intell. Transp. Syst.*, vol. 6, no. 3, pp. 314–325, Sep. 2005.

[2] J. J. Martinez and C. Canudas-de-Wi, "A safe longitudinal control for adaptive cruise control and stop-and-go scenarios," *IEEE Trans. Control Syst. Technol.*, vol. 15, no. 2, pp. 246–258, Mar. 2007.

[3] E. Adell, A. Várhelyi, and M. D. Fontana, "The effects of a driver assistance system for safe speed and safe distance—A real-life field study," *Transp. Res. C, Emerg. Technol.*, vol. 19, pp. 145–155, Feb. 2011.

[4] D. Pan, Y. Zheng, J. Qiu, and L. Zhao, "Synchronous control of vehicle following behavior and distance under the safe and efficient steady-following state: Two case studies of high-speed train following control," *IEEE Trans. Intell. Transp. Syst.*, vol. 19, no. 5, pp. 1445–1456, May 2018.

[5] H. M. Zhang and T. Kim, "A car-following theory for multiphase vehicular traffic flow," *Transp. Res. B, Methodol.*, vol. 39, no. 5, pp. 385–399, Jun. 2005.

[6] T. Tang, Y. Wang, X. Yang, and Y. Wu, "A new car-following model accounting for varying road condition," *Nonlinear Dyn.*, vol. 70, pp. 1397–1405, Oct. 2012.

[7] Y.-X. Huang *et al.*, "Experimental study and modeling of car-following behavior under high speed situation," *Transp. Res. C, Emerg. Technol.*, vol. 97, pp. 194–215, Dec. 2018.

[8] M. Brackstone, B. Sultan, and M. McDonald, "Motorway driver behaviour: Studies on car following," *Transp. Res. F, Traffic Psychol. Behav.*, vol. 5, no. 1, pp. 31–46, Mar. 2002.

[9] S. Ossen and S. P. Hoogendoorn, "Driver heterogeneity in car following and its impact on modeling traffic dynamics," *Transp. Res. Rec.*, vol. 1, no. 1999, pp. 95–103, Jan. 2007.

[10] B. Gunay, "Car following theory with lateral discomfort," *Transp. Res. B, Methodol.*, vol. 41, no. 7, pp. 722–735, Aug. 2007.

[11] B. Ponnu and B. Coifman, "Speed-spacing dependency on relative speed from the adjacent lane: New insights for car following models," *Transp. Res. B, Methodol.*, vol. 82, pp. 74–90, Dec. 2015.

[12] S. Lei and L. Huapu, "Model of vehicle behavior under multilane road conditions," *J.-Huazhong Univ. Sci. Technol. Nature Sci. Ed.*, vol. 35, no. 6, pp. 115–117, Jun. 2007.

[13] X. Ma and I. Andreasson, "Behavior measurement, analysis, and regime classification in car following," *IEEE Trans. Intell. Transp. Syst.*, vol. 8, no. 1, pp. 144–156, Mar. 2007.

[14] W. Xuesong, Y. Minming, and D. Hurwitz, "Analysis of cut-in behavior based on naturalistic driving data," *Accident Anal. Prevention*, vol. 124, pp. 127–137, Mar. 2019.

[15] D. Zhao, X. Huang, H. Peng, H. Lam, and D. J. LeBlanc, "Accelerated evaluation of automated vehicles in car-following maneuvers," *IEEE Trans. Intell. Transp. Syst.*, vol. 19, no. 3, pp. 733–744, May 2017.

[16] R. Jiang, M.-B. Hu, H. M. Zhang, Z. Y. Gao, and Q.-S. Wu, "On some experimental features of car-following behavior and how to model them," *Transp. Res. B, Methodol.*, vol. 80, pp. 338–354, Oct. 2015.

[17] R. Schmied, H. Waschl, and L. del Re, "Comfort oriented robust adaptive cruise control in multi-lane traffic conditions," *IFAC-PapersOnLine*, vol. 49, no. 11, pp. 196–201, Aug. 2016.

[18] L. Li, D. Zhang, Z.-G. Xu, P. Wang, and G.-P. Wang, "The roles of car following and lane changing drivers' anticipations during vehicle inserting process: a structural equation model approach," *J. Adv. Transp.*, vol. 2018, Nov. 2018, Art. no. 6372861.

[19] S. Moon, H. J. Kang, and K. Yi, "Multi-vehicle target selection for adaptive cruise control," *Vehicle Syst. Dyn.*, vol. 48, no. 11, pp. 1343–1352, Oct. 2010.

[20] N. Deo and M. M. Trivedi, "Multi-modal trajectory prediction of surrounding vehicles with maneuver based LSTMs," in *Proc. IEEE Intell. Vehicles Symp. (IV)*, Jun. 2018, pp. 1179–1184.

[21] S. Moon, I. Moon, and K. Yi, "Design, tuning, and evaluation of a full-range adaptive cruise control system with collision avoidance," *Control Eng. Pract.*, vol. 17, no. 4, pp. 442–455, Apr. 2009.

[22] S. Vogel, H. Ney, and C. Tillmann, "HMM-based word alignment in statistical translation," in *Proc. 16th Conf. Comput. Linguistics*, vol. 2, Aug. 1996, pp. 307–313.

[23] Y. Hu, W. Zhan, and M. Tomizuka, "Probabilistic prediction of vehicle semantic intention and motion," in *Proc. IEEE Intell. Vehicles Symp. (IV)*, Jun. 2018, pp. 307–313.

[24] V. Gadepally, A. Krishnamurthy, and U. Ozguner, "A framework for estimating driver decisions near intersections," *IEEE Trans. Intell. Transp. Syst.*, vol. 15, no. 2, pp. 637–646, Apr. 2014.

[25] M. T. Parker, "Effect of heavy goods vehicles and following behaviour on capacity at motorway roadwork sites," *Traffic Eng. Control*, vol. 37, no. 9, pp. 524–531, Sep. 1996.

[26] W. van Winsum and W. Brouwer, "Time headway in car following and operational performance during unexpected braking," *Perceptual Motor Skills*, vol. 84, no. 3, pp. 1247–1257, Jun. 1997.

[27] K. H. Zou, K. Tuncali, and S. G. Silverman, "Correlation and simple linear regression," *Radiology*, vol. 227, no. 3, pp. 617–628, Jun. 2003.

[28] K.-Y. Liang and S. L. Zeger, "Longitudinal data analysis using generalized linear models," *Biometrika*, vol. 73, no. 1, pp. 13–22, Apr. 1986.

[29] R. M. O'brien, "A caution regarding rules of thumb for variance inflation factors," *Qual. Quantity*, vol. 41, no. 5, pp. 673–690, Oct. 2007.

[30] T. A. Craney and J. G. Surles, "Model-dependent variance inflation factor cutoff values," *Qual. Eng.*, vol. 14, no. 3, pp. 391–403, Feb. 2002.

[31] B. T. Morris and M. M. Trivedi, "Learning, modeling, and classification of vehicle track patterns from live video," *IEEE Trans. Intell. Transp. Syst.*, vol. 9, no. 3, pp. 425–437, Sep. 2008.

[32] S. B. Amsalu, A. Homaifar, F. Afghah, S. Ramyar, and A. Kurt, "Driver behavior modeling near intersections using support vector machines based on statistical feature extraction," in *Proc. IEEE Intell. Vehicles Symp. (IV)*, Jun./Jul. 2015, pp. 1270–1275.

[33] C. Fraley and A. E. Raftery, "Model-based clustering, discriminant analysis, and density estimation," *J. Amer. Stat. Assoc.*, vol. 97, no. 458, pp. 611–631, Jun. 2002.

[34] T. V. Gestel, J. A. Sukens, G. Lanckriet, A. Lambrechts, B. De Moor, and J. Vandewalle, "Bayesian framework for least-squares support vector machine classifiers, Gaussian processes, and kernel Fisher discriminant analysis," *Neural Comput.*, vol. 14, no. 5, pp. 1115–1147, May 2002.

[35] W. Yuan, R. Fu, and Y. Ma, "A study on driver's vehicle-following model based on high speed real driving data," *Auto Eng.*, vol. 37, no. 6, pp. 679–685, Jun. 2015.
[36] W. Chang, F. Rui, G. Yingshi, and Y. Wei, "Prediction method of time-to-line-crossing in lane change warning system," *Auto Eng.*, vol. 36, no. 4, pp. 509–514, Jun. 2014.
[37] W. Chang, S. Qinyu, F. Rui, L. Zhen, and Z. Qiong, "Lane change warning threshold based on driver perception characteristics," *Accident Anal. Prevention*, vol. 117, pp. 164–174, Aug. 2018.
[38] H. Bellem, M. Klüver, M. Schrauf, H. P, Schöner, H. Hecht, and J. F. Krems, "Can we study autonomous driving comfort in moving-base driving simulators? A validation study," *Hum. Factors*, vol. 59, pp. 442–456, May 2017.

YINGSHI GUO received the B.Tech. and M.S. degrees in vehicle application engineering from the Jilin University of Technology, Changchun, China, in 1985 and 2000 respectively, and the Ph.D. degree in vehicle engineering from Chang'an University, Xi'an, China, in 2009.

He is currently a Professor with the Department of Vehicle Engineering, School of Automobile, Chang'an University. His research interests include automobile test technology, human-machine systems, vehicle control, and vehicle active safety.

QINYU SUN received the B.Tech. and M.S. degrees in vehicle engineering from the Xi'an University of Science and Technology, Xi'an, China, in 2013 and 2016, respectively. He is currently pursuing the Ph.D. degree in vehicle engineering with the School of Automobile, Chang'an University. His research interests include autonomous driving, human-machine collaboration control, and vehicle active safety.

RUI FU received the B.Tech., M.S., and Ph.D. degrees in vehicle application engineering from the Jilin University of Technology, Changchun, China, in 1985, 1989, and 1996, respectively.

She is currently a Professor with the Department of Transportation Safety, School of Automobile, Chang'an University. Her research interests include human factors, driving behavior, human-machine collaboration control, and vehicle active safety.

CHANG WANG received the B.Tech., M.S., and Ph.D. degrees in transportation safety engineering from Chang'an University, Xi'an, China, in 2005, 2009, and 2012, respectively.

He is currently an Associate Professor with the Department of Transportation Safety Engineering, School of Automobile, Chang'an University. His research interests include traffic optimization, driving behavior, and vehicle active safety.